

## Influence of manganese chloride filler on optical and structural properties of PVA/PVP films

E.M.Abdelrazek<sup>1</sup>, A.M.Abdelghany<sup>2</sup>, A.A.Aldhabi<sup>1\*</sup>

<sup>1</sup>Physics Dept., Faculty of Science, Mansoura University, Mansoura, 35516, (EGYPT)

<sup>2</sup>Spectroscopy Dept., Physics Division, National Research Center, Cairo, 12311, (EGYPT)

E-mail: a.m\_abdelghany@yahoo.com

### ABSTRACT

Films of Poly (vinyl alcohol) (PVA)/ Poly (vinyl pyrrolidone) (PVP) polyblend filled of  $MnCl_2$  were prepared by using the casting technique. The amorphous feature of the filled polymer was depicted using XRD. The area under the peak and peak intensity was found to decrease with increasing  $MnCl_2$  concentration due to the interaction between the polymer blend and  $MnCl_2$ ; this indicates decreasing in the degree of crystallinity in the polymeric matrix. Fourier transform infrared spectroscopy display significant structural changes within the polymeric matrix indicating a complexation between the pristine polymer and the filler. UV-Vis. optical absorption spectrum indicates a variation in both intensity and optical energy gap with different amount of filler. Both values of direct and indirect energy gaps are calculated and discussed. Obtained data shows a defect formation which increases filler content and supported by both XRD and UV-Vis. Data. Scanning electron microscopy (SEM) shows a homogenous distribution of the filler within the polymeric matrix and in the filled films with different concentrations of  $MnCl_2$  appear a large granules and granule groups randomly distribution on the surface this indicates that these granules may be are of  $MnCl_2$ . © 2013 Trade Science Inc. - INDIA

### KEYWORDS

XRD;  
FTIR;  
UV-Vis.;  
SEM;  
Polymer blend;  
 $MnCl_2$

### INTRODUCTION

Polymer materials are of present interest because, in combination with suitable metal salts, they give matrix which is useful for the development of advanced high-energy electrochemical devices, e.g. batteries, fuel cells, electrochemical display devices, and photo electrochemical cells. The main advantages of polymeric matrix are their good mechanical properties, ease of

fabrication into thin films of desirable size<sup>[1]</sup>. Polyvinyl alcohol (PVA) has different internal structures, which may be considered as amorphous or semicrystalline. The semicrystalline structure of PVA showed an important feature rather than of amorphous one. This is because semicrystalline PVA leads to the formation of both crystalline and amorphous regions. Moreover, PVA is also nontoxic, potential material having high dielectric strength, good charge storage capacity and dopant

## Full Paper

dependent electrical and optical properties<sup>[2]</sup>. Polyvinyl pyrrolidone (PVP) deserves special attention among the conjugated polymers because of its good environmental stability, easy processability, moderate electrical conductivity, and rich physics in charge transport mechanism. The local modification of the chemical structure induces drastic changes in electronic properties<sup>[3]</sup>. PVP/PVA interactions have been described in many papers because of interesting properties of the resulting blend, which combines the features of both polymers<sup>[4]</sup>. The blending of different polymers or inorganic particles with polymers represents a strategic route to improve the performance of a material, allow realization of novel composite systems that enhance the performance of the parent polymer<sup>[5]</sup>.

PVP/PVA blend is mainly applied in medicine as a skin dressing component and electrochemical as membranes<sup>[6]</sup>. Filler additives were added to polymer or polymer blend to improve and modify its properties. Transition metals have influence on the structural, optical, morphological of polymer blend. And little systematic investigations have been carried out in this field, especially on the particulate composite systems.  $MnCl_2$  is used in polymers for a variety of reasons: cost reduction, improved processing, density control, optical effect, thermal conductivity, control of thermal expansion, electrical properties, etc. Both PVP and PVA are water-soluble and miscible in all proportions. The structural, optical, and electrical properties of blends can be suitably modified by the addition of the fillers depending on their reactivity with the host matrix<sup>[7]</sup>. In the present work, PVA/PVP (50/50) blend filled with different concentrations of  $MnCl_2$  have been prepared by casting method, and was study influence of  $MnCl_2$  as filler on the physical properties.

## MATERIAL AND EXPERIMENTAL WORK

### Materials

Polyvinyl alcohol (PVA) of molecular weight 14000 and polyvinyl pyrrolidone (PVP) of molecular weight 40,000 gm/mol supplied by Merck, Germany, were used as a basic polymeric materials.  $MnCl_2$  supplied by Hayashi pure chemical industries, Ltd. Japan were provided in powder state and used without further purification.

Pure blend of PVA/ PVP (50/50) with and without filler of  $MnCl_2$  were prepared by the casting method technique. Water was used to dissolve the polymeric matrix and filler of  $MnCl_2$  with constant stirring at 50°C to complete dissolution. The mixture was stirred for four hours until a complete dissolution of polymeric matrix and metal halide achieved and a suitable viscous solution is formed. The final viscous solution were poured onto cleaned Petri dishes and dried in an oven at 50°C for 5 days to remove the solvent traces. After drying, the films were peeled from Petri dishes and kept in vacuum desiccators until use. Calculated masses of PVA/PVP and filler mass fractions (0.0, 5, 10, 20, 25 and 30 wt %) of  $MnCl_2$  were prepared according to :

$$W \text{ (wt\%)} = \frac{W_f}{W_f + W_p} \times 100$$

Where  $w_f$  and  $w_p$  represent the weights of the filler and polymer, respectively.

### Characterization techniques

X-ray diffraction (XRD) scans were obtained using PANalytical X'Pert PRO XRD system using Cu K $\alpha$  radiation (where,  $\lambda = 1.540 \text{ \AA}$ , the tube operated at 30 kV, the Bragg's angle ( $2\theta$ ) in the range of 10–60 degree. Fourier Transform Infrared (FTIR) measurements were carried out using single beam Fourier transform-infrared spectrometer (Nicolet iS10, USA) at room temperature in the spectral range from 4000–400  $cm^{-1}$ . UV/Vis. absorption spectra were measured in the wavelength region of 200–800 nm using spectrophotometer (V-570 UV/VIS/NIR, JASCO, Japan) to study the change in structures of the samples due to the addition of the filler and their optical properties. The morphology of the films was characterized by scanning electron microscopy using (Quanta FEG 250), operating at 200V–30 kV accelerating voltage magnification 14x up to 5000x. Surfaces of the samples were coated with a thin layer of gold (3.5 nm) by the vacuum evaporation technique to minimize sample charging effects due to the electron beam.

## RESULTS AND DISCUSSIONS

### X-ray diffraction analysis (XRD)

Figure 1 shows the X-ray diffraction scans of pure

PVA/PVP blend and the blend filled with different concentrations of  $\text{MnCl}_2$  as filler. The observed spectra exhibit an amorphous feature and shows broad band at about  $2\theta = 20^\circ$ . The area under the peak and peak intensity was found to decrease with increasing  $\text{MnCl}_2$  concentration due to the interaction between the polymer blend and  $\text{MnCl}_2$  as show in Figure 2. This implies a decrease in the degree of crystallinity and causes an increase in the amorphous regions this indicated that an intermolecular hydrogen bonding interaction occurred

between the blend and  $\text{MnCl}_2$ ; this reveals the semi-crystalline nature of the blend that contains crystalline and amorphous structure<sup>[8]</sup>. This behavior demonstrates that complexation between the filler and polymer blend took place in the amorphous regions. Also the change of the peaks position in the filled samples this indicates the complexation between the polymers blend and  $\text{MnCl}_2$ , and that the filler significantly influence of the degree of crystallinity and produce more defects in the polymeric matrix<sup>[9]</sup>.

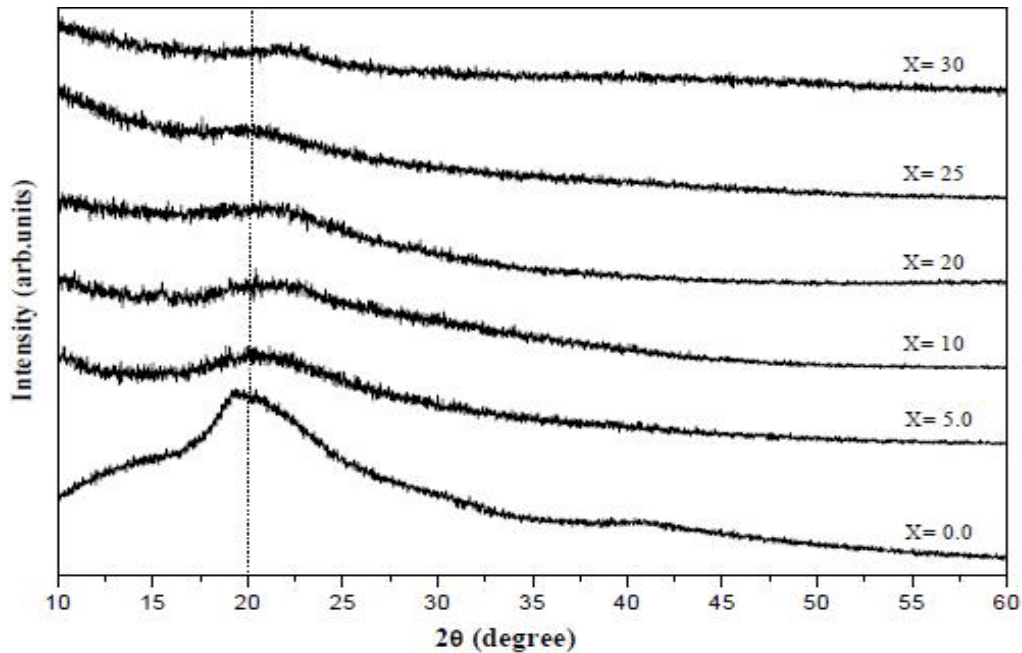


Figure 1 : X-ray diffraction scans of PVA/PVP blend with different mass fractions of  $\text{MnCl}_2$  %.

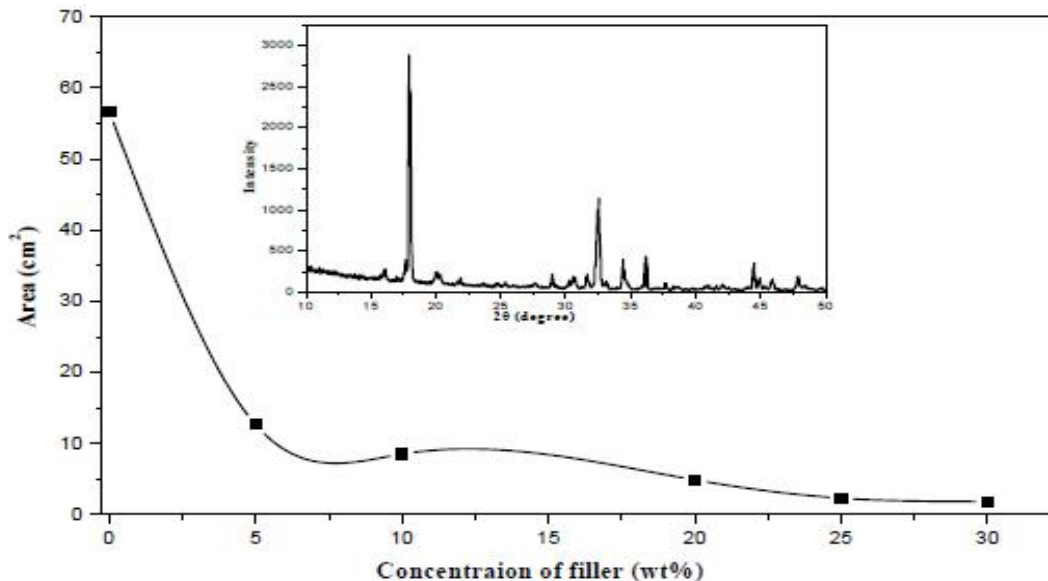


Figure 2 : Relation between filler concentration (wt %) versus peak area and the X-ray diffraction scans for the crystalline phases pure of  $\text{MnCl}_2$ .

## Full Paper

### Fourier transforms infrared absorption spectra (FTIR)

A Fourier transform infrared spectrum was employed for structural characterization of PVA/PVP blend films without and with different concentrations of  $\text{MnCl}_2$ . Figure 3 shows FT-IR absorption spectra exhibit bands characteristic of stretching and bending vibrations of the films. From the spectra, we observed broad band at about  $3380\text{ cm}^{-1}$  is assigned to O–H stretching vibration of hydroxyl group which is the most characteristic band of alcohols<sup>[8-10]</sup>. The band corresponding to methylene group ( $\text{CH}_2$ ) asymmetric stretching vibration occurs at about  $2950\text{ cm}^{-1}$ <sup>[9,11]</sup>. The band absorption at

TABLE 1: FTIR peak assignment of pure and filled of PVA/PVP

Vibrational Frequency (cm-1)	Band assignment	References
3380	O–H stretching	8, 9, 10
2950	$\text{CH}_2$ asymmetric stretching	9, 11
1740	C=O stretching	8, 12
1620	C=C stretching	10, 13
1463	O–H bending	8, 11
1440	C=C pyridine ring	8, 14
1377	C–H bending	10
1295	C–O stretching	14, 15
1094	C–O stretching	9, 11
840	C–C stretching	8, 9

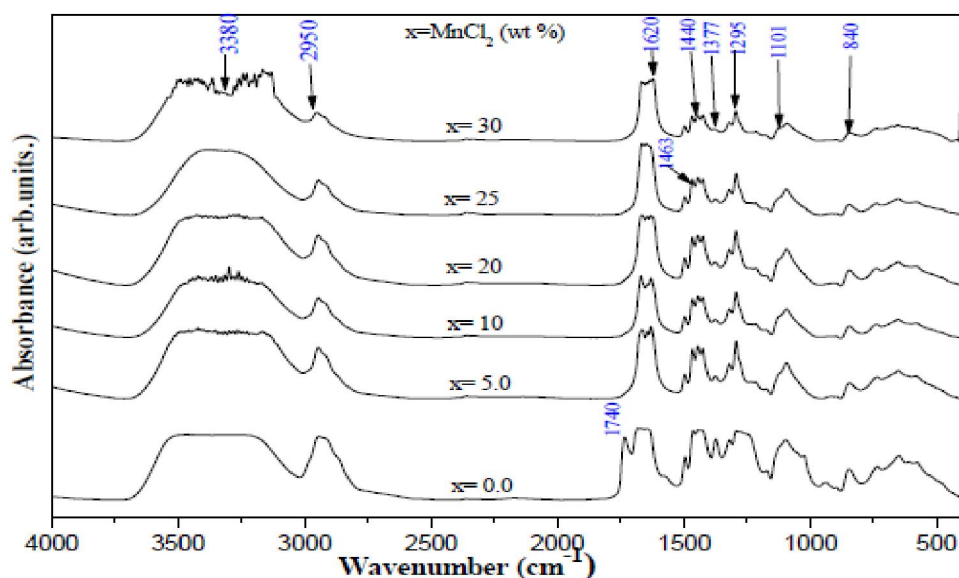


Figure 3 : FT-IR of PVA/PVP blend and blend with different mass fractions of  $\text{MnCl}_2$  %.

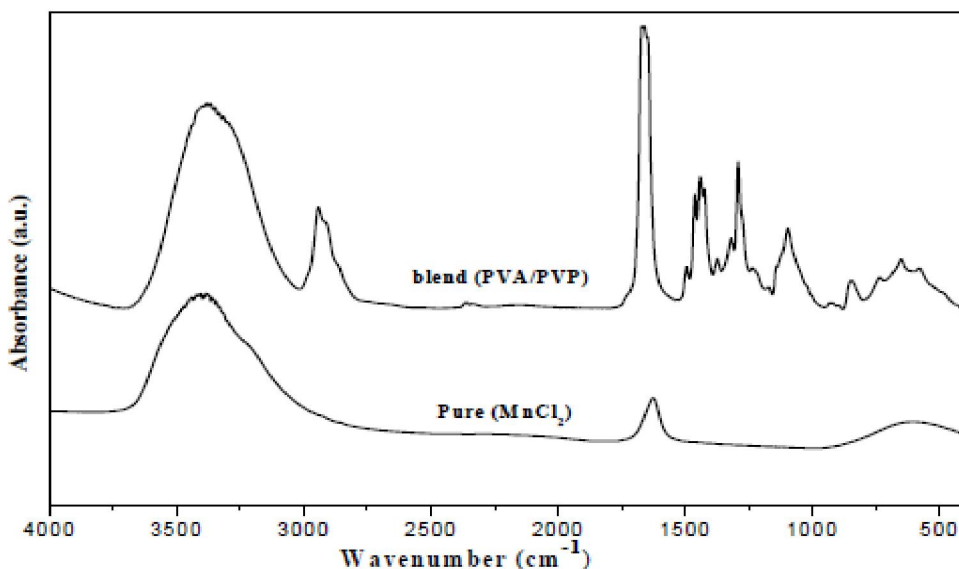


Figure 4 : FT-IR spectrum of pure  $\text{MnCl}_2$  and blend (PVA/PVP)

about  $1740\text{ cm}^{-1}$  C=O stretching was observed<sup>[8,12]</sup>, and also this peak occur shift to  $1685\text{ cm}^{-1}$  with add the filler; this suggests a complexation between the polymer and the filler. And the band at  $1620\text{ cm}^{-1}$  C=C stretching has confirmed the semicrystalline nature of the blends<sup>[10,13]</sup>. The appearance at  $1463\text{ cm}^{-1}$ , which assigned to O–H bending<sup>[8,11]</sup>, the band at about  $1440\text{ cm}^{-1}$  corresponds to C=C pyridine ring<sup>[8,14]</sup>, and occurs decrease in the intensity of peak with increase the filler. And the band absorption at about  $1377\text{ cm}^{-1}$  was assigned to C–H bending<sup>[10]</sup>. The vibrational band at about  $1295\text{ cm}^{-1}$  corresponds to C–O stretching of acetyl groups present on the PVA backbone<sup>[14,15]</sup>. All previously mentioned results confirm the occurrence of complexation between the polymer blend and  $\text{MnCl}_2$ . Detailed assignments were presented in TABLE 1.

### UV-Vis. Optical studies (UV-Vis.)

UV–Vis. spectra in the wavelength range of 200–800 nm at room temperature of the PVA/PVP filled with various concentration of  $\text{MnCl}_2$ . The changes in the transmitted radiation can decide the types of possible electron transitions. From Figure 5 we can observed spectra are characterized by the main absorp-

tion edge around 233 nm for all curves that shifted towards longer wavelengths with increasing  $\text{MnCl}_2$  content. These shifts indicate the complexation between the filler and the polymer blend and may be also attributed to change in crystallinity due to filler adding<sup>[16,17]</sup>. The absorption bands are due to electronic transition from the ground states to excited states. During such transition in a molecule, electrons are promoted from the highest occupied molecular orbital (HOMO) to the lowest unoccupied molecular orbital (LUMO)<sup>[18]</sup>.

Figure 5. shows absorption edge at 233 nm and are assigned to localized  $\pi \rightarrow \pi^*$  transitions<sup>[8,9,14,19]</sup> which comes from unsaturated bonds, mainly; carbonyl groups (C=O and/or C=C)<sup>[20,21]</sup>, which is responsible for electrical conduction in the samples which observed in FT-IR at about  $1740\text{ cm}^{-1}$  and  $1620\text{ cm}^{-1}$ .

### Determination of optical energy gap (Eg)

The study of optical absorption gives information about the band structure of organic compound. In the absorption process an electron is excited from a lower to higher energy state by absorbing a photon of known energy. The changes in the transmitted radiation can decide the types of possible electron transitions. Fundamental absorption refers to band-to-band or

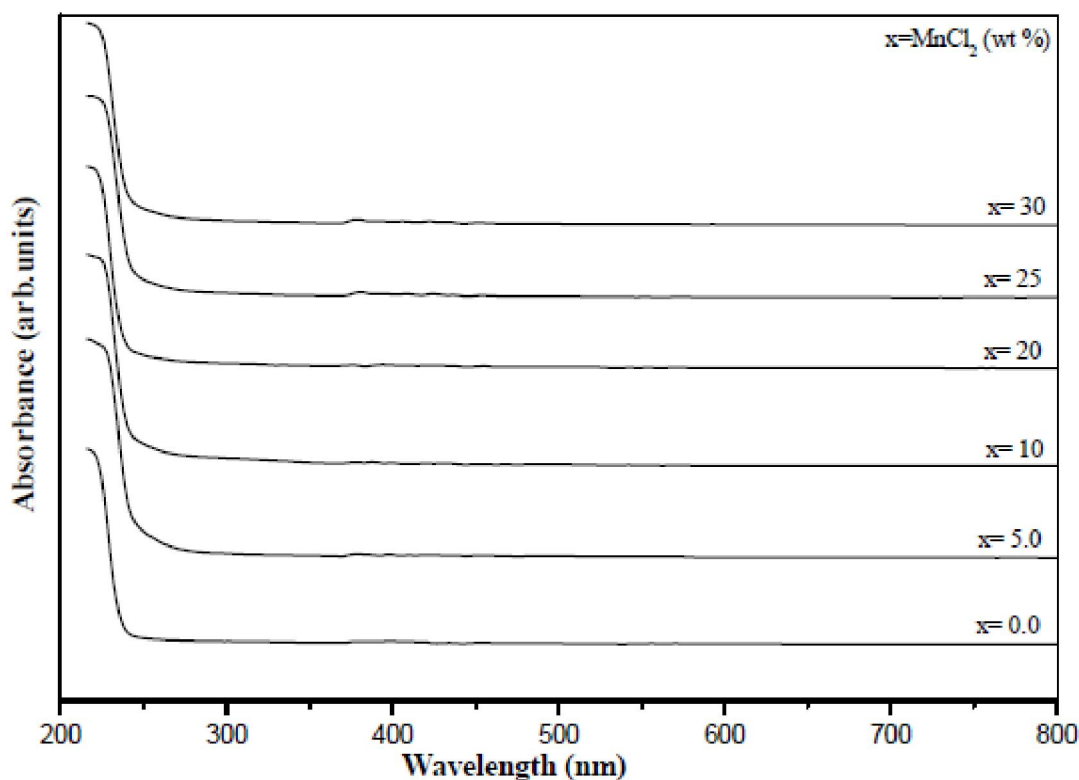


Figure 5 : UV/Vis. spectra of pure PVA/PVP blend and the blend filled with different concentrations of  $\text{MnCl}_2$  wt%

## Full Paper

exciting transition. The fundamental absorption shows a sudden rise in absorption, known as absorption edge, which can be used to determine the optical band gap

( $E_g = h c/\lambda$ ). Absorption is expressed in terms of a coefficient  $\alpha$ , which is defined as the relative rate of decrease in light intensity.

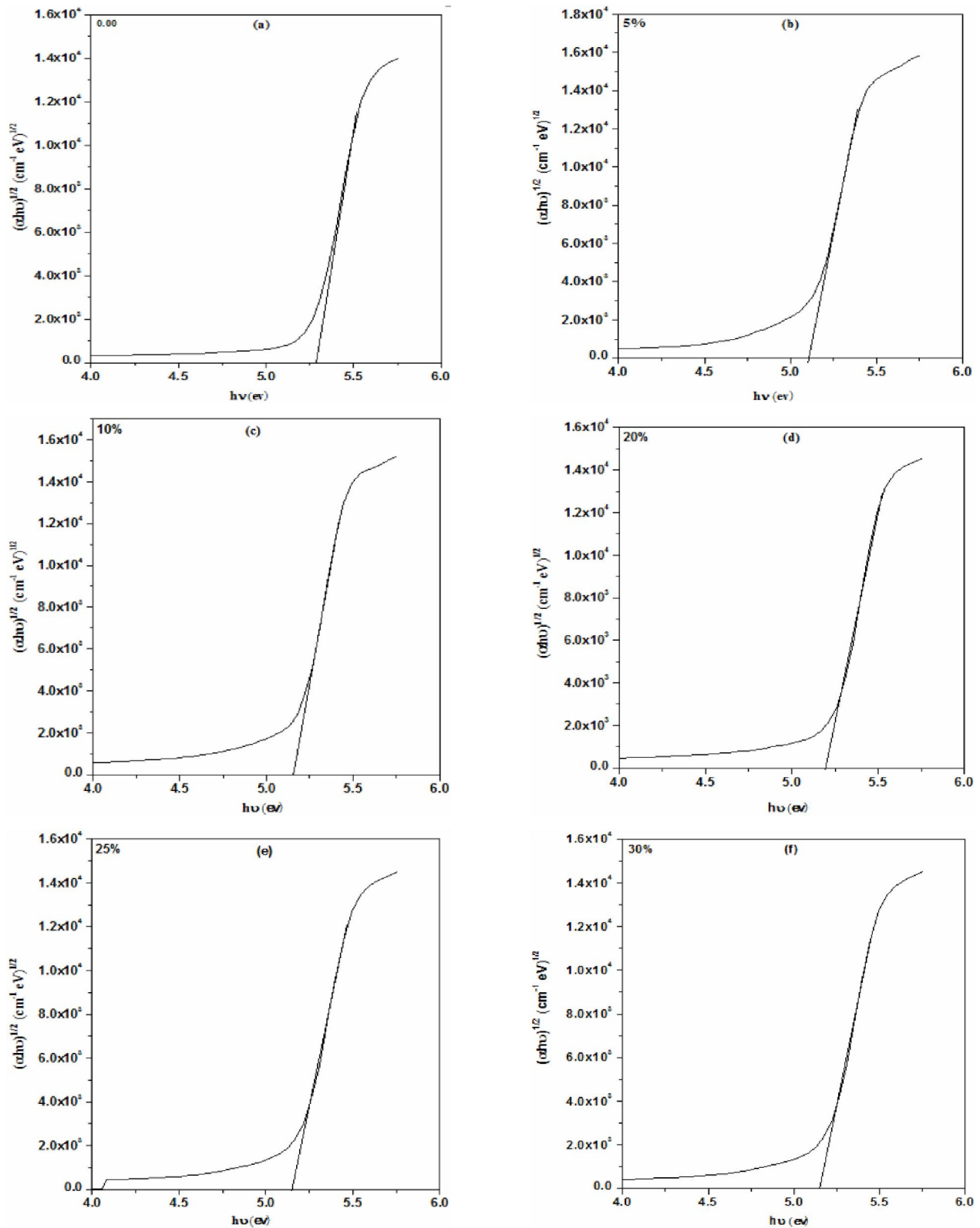


Figure 6 : (a-f) The relation between  $(\alpha hu)^{1/2}$  versus photon energy ( $hu$ )

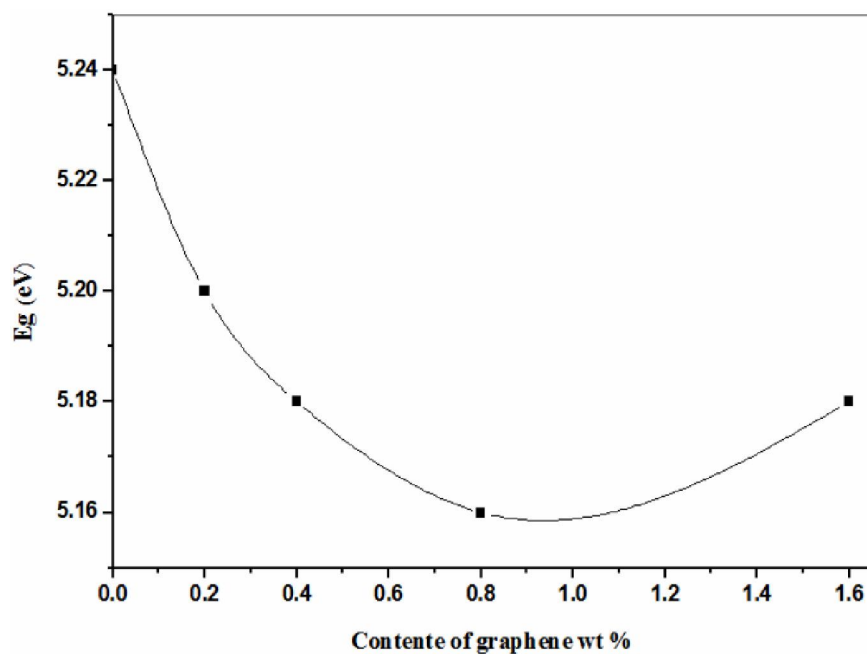
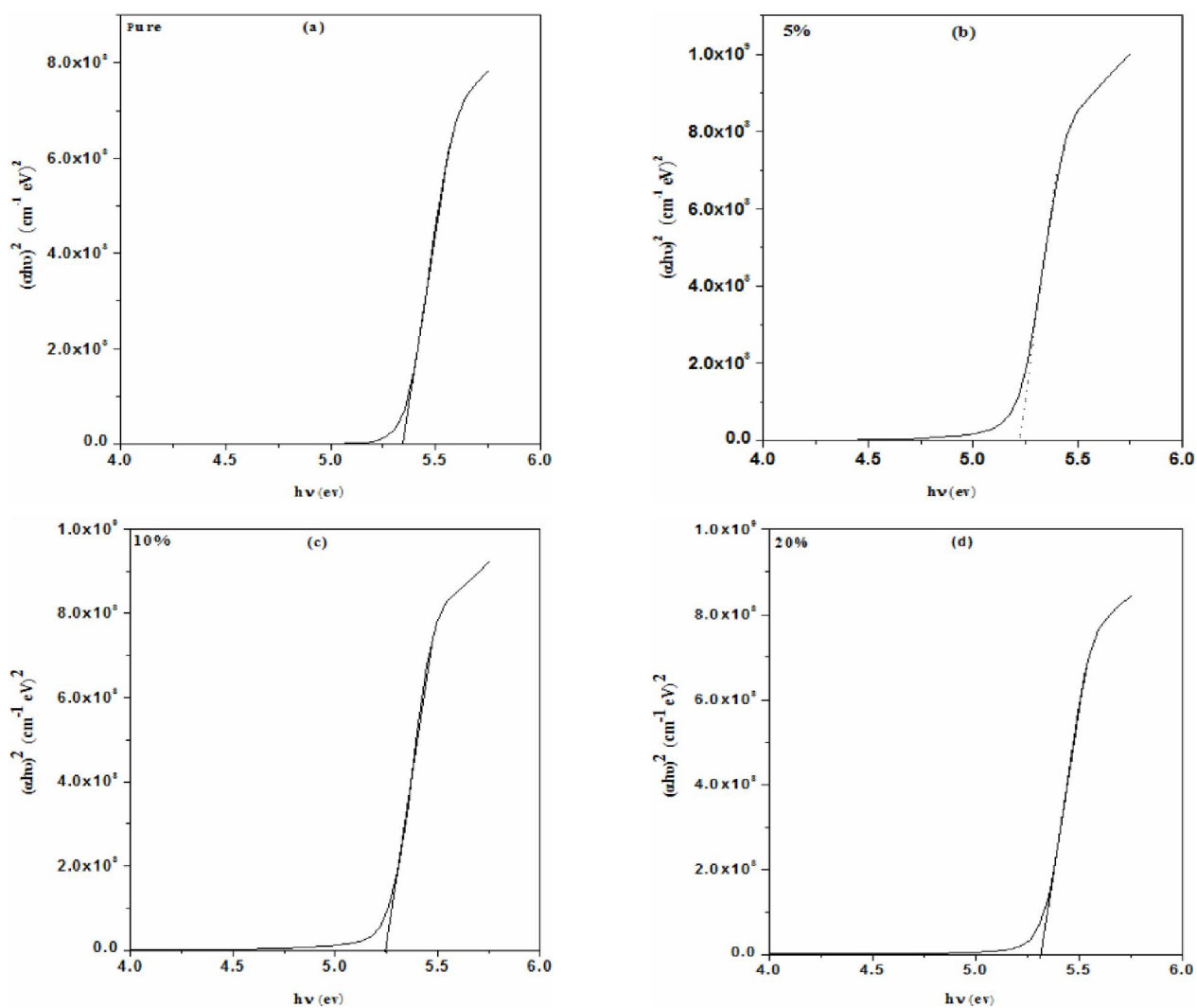


Figure 6.a : The relation between optical energy gap ( $E_g$ ) with concentrations wt %



## Full Paper

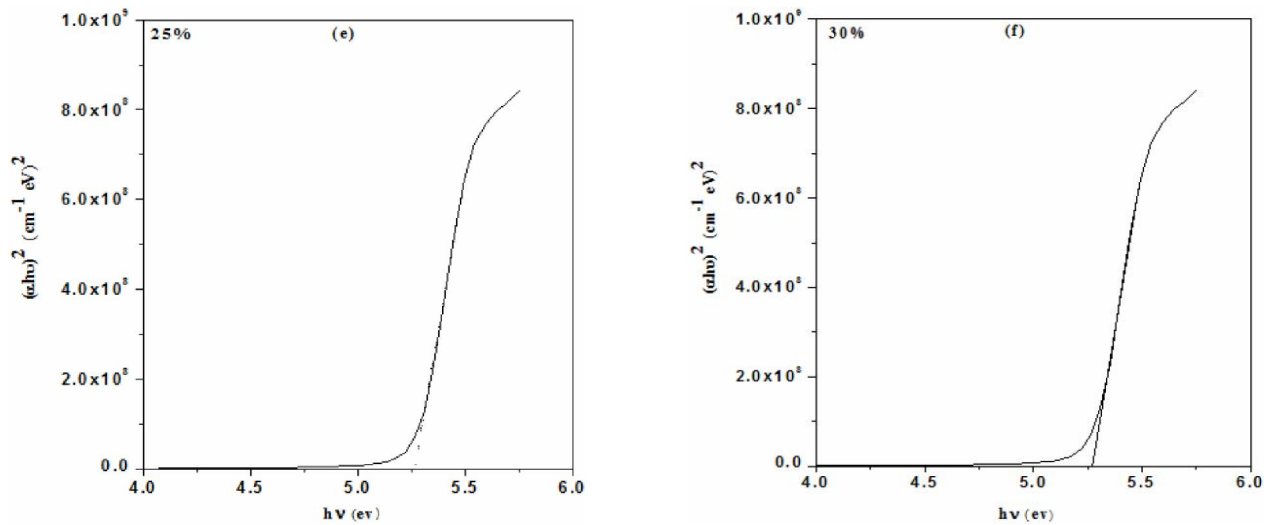
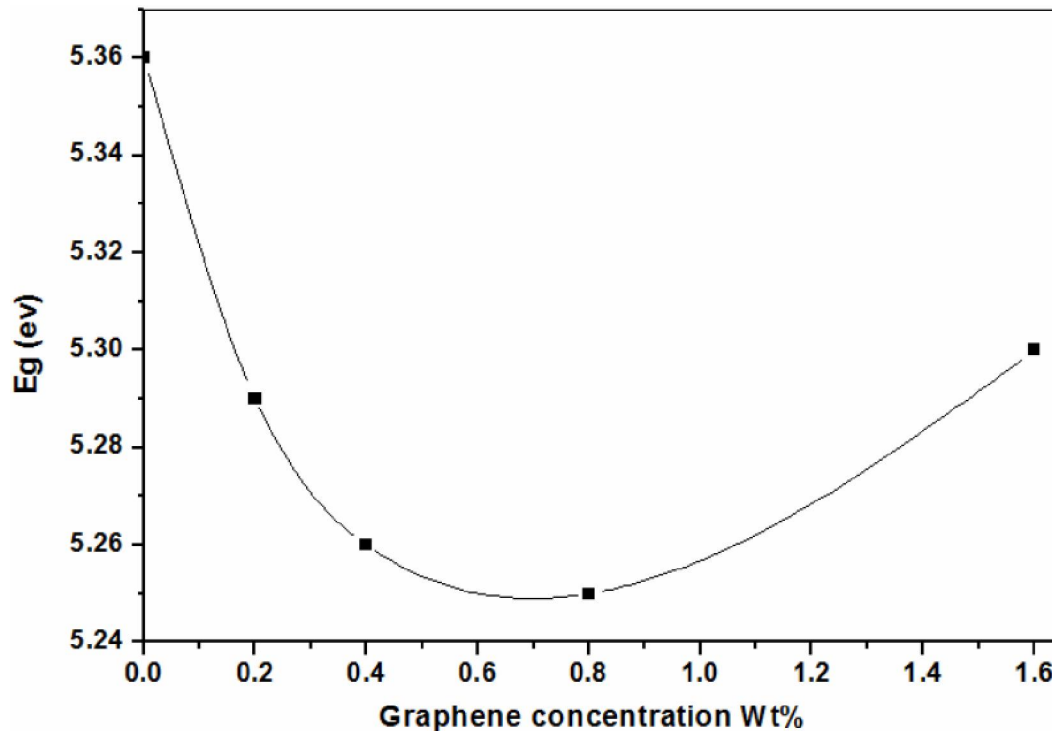
Figure 7(a-f) : The relation between  $(\alpha hv)^2$  versus photon energy ( $h\nu$ )Figure 7.a : The relation between  $E_g$  (eV) with content of filler (wt %).

TABLE 2 : Relation between content filler, degree of crystallinity and Optical Energy gap for direct and indirect with content filler in PVA/PVP blend films.

Content of MnCl <sub>2</sub> (wt %)	Degree of Crystallinity %	Optical Energy gap (eV)	
		Direct	Indirect
0.0	3.50	5.34	5.29
5.0	3.15	3.24	5.17
10	2.91	5.23	5.16
20	2.83	5.31	5.19
25	2.79	5.26	5.15
30	2.71	5.26	5.13

The analysis of Thutupalli and Tomlin<sup>[22]</sup> is based on the following relations:

$$(n\alpha hv)^2 = C_1(h\nu - E_{gd}) \quad (1)$$

$$(n\alpha hv)^{\frac{1}{2}} = C_2(h\nu - E_{gi}) \quad (2)$$

where,  $h\nu$  is the photon energy,  $E_{gd}$ , the direct band gap,  $E_{gi}$ , the indirect band gap,  $n$ , integer,  $C_1$ ,  $C_2$ , constants and  $\alpha$  is the absorption coefficient. The absorption coefficient ( $\alpha$ ) can be determined as a function of frequency using the formula<sup>[23]</sup>:



**TABLE 3 :Symbols and the equal of concentration of MnCl<sub>2</sub> in the films PVA/PVP**

Name	Concentration wt %
S-0	0.0
S-1	5.0
S-2	10
S-3	20
S-4	25
S-5	30

$$\alpha(\nu) = 2.303 \times \frac{A}{d} \quad (3)$$

where, A is the absorbance and d is thickness of the sample under investigation. Davis and Shalliday<sup>[24]</sup> reported that near the fundamental band edge, both direct and indirect transitions occur and can be observed by plotting  $(\alpha h\nu)^2$  and  $(\alpha h\nu)^{1/2}$ , respectively, as a function of energy ( $h\nu$ ), where h is Planck's constant. Figure 6 and Figure 7 show the plots of

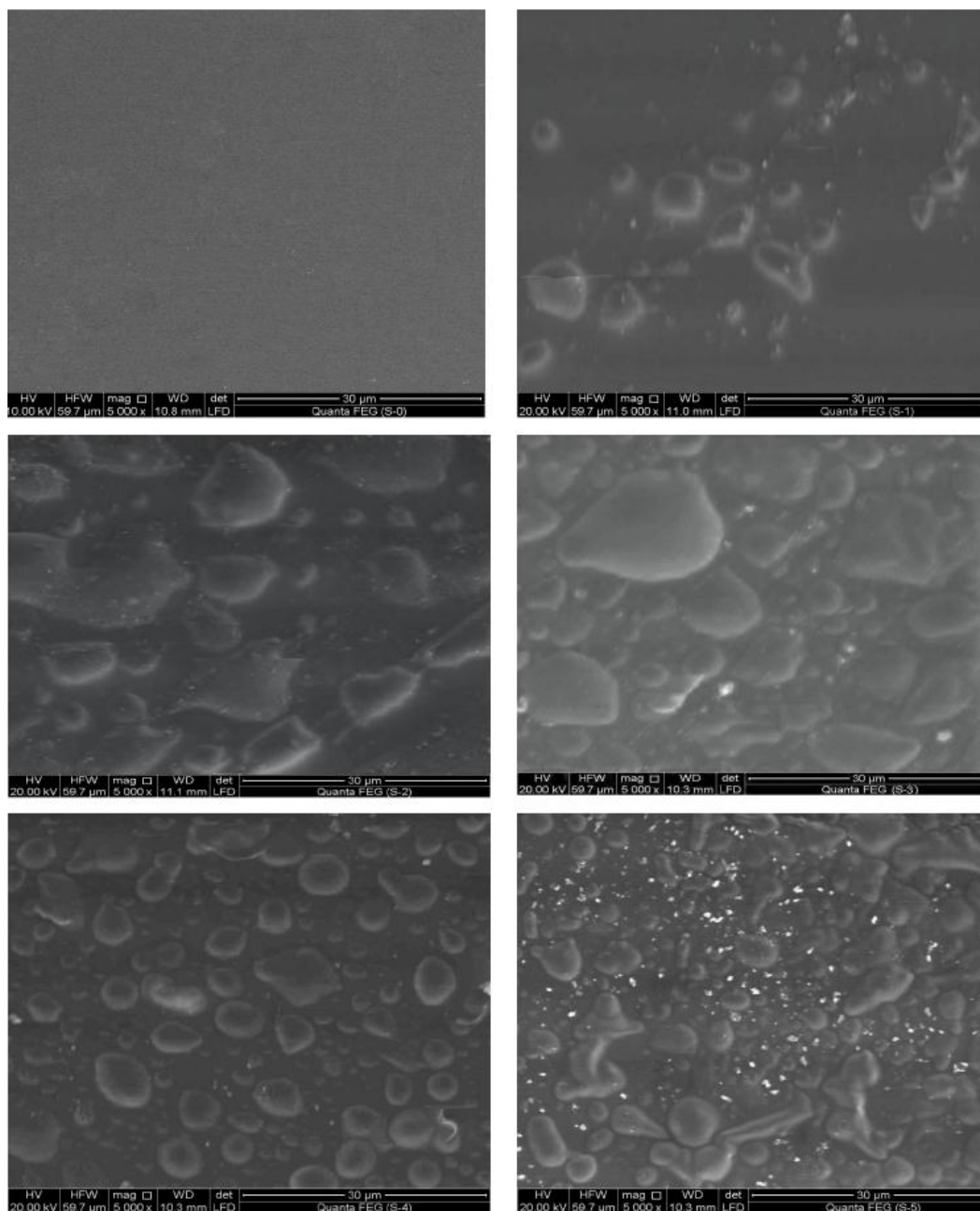


**Figure 8: SEM micrograph of the surface of: pure blend, 5, 10, 20, 25 and 30 wt % of different concentrations of MnCl<sub>2</sub> at magnification 5000 times.**

## Full Paper

$(\alpha h\nu)^{1/2}$  and  $(\alpha h\nu)^2$  respectively, as a function of photon energy ( $h\nu$ ), and can be used to calculate its optical energy gap; these obtained values are listed in TABLE 2. The nature and width of the band gaps can be evaluated from both Figure 6 and Figure 7 and absorption edge values were obtained by extrapolating the linear portions. The values of indirect band gap and direct band gap are listed in TABLE 2 and showed in both (Figure 6.a) and (Figure 7.a). It is clear from TABLE 2 and the Figures that the indirect and direct band gap values showed a decrease with increasing  $\text{MnCl}_2$  content. This decrease may be attributed to the formation of defects in the polymeric matrix and an increase in the degree of disorder in the films. These defects produce the localized states in the optical band gap. These overlaps are responsible for decreasing energy band gap when content  $\text{MnCl}_2$  is increased in the polymer matrix<sup>[25]</sup>. These results are supported by the data obtained from XRD studies.

### Scanning electron microscopy

Morphology of the studied samples was investigated with SEM to provide further information about the structural modifications of PVA/PVP blend films due to filling with  $\text{MnCl}_2$ . Figure 8 shows the SEM micrograph of the surface of pure blend and filled films with different concentrations of  $\text{MnCl}_2$  at magnification 5000 times, and shows pure polymer morphology which is transparent and is shown to be in a uniform morphology revealing a rather smooth surface. By increasing the concentration of  $\text{MnCl}_2$  appear a large granules and granule groups randomly distribution on the surface. The grown ones were of different sizes and irregular shapes, uniformly distributed in the amorphous matrix, and the number of the granules increases with increasing concentration of  $\text{MnCl}_2$ , this indicates that these granules may be are of  $\text{MnCl}_2$ , and indicating the occurrence of a homogeneous growth mechanism. An interesting pattern is observed for the case of  $w=30$  wt % which contains an aggregation of filler and a highly condensed number of very small granules at the surface, because access to the state of saturation as in figure 8 and this confirmed the complexation between the filler and the polymer blend and attributed to the partial compatibility between the polymer blend and the filler.

These results confirm measurements of XRD and UV/Vis. Measurements.

### CONCLUSION

Polymer electrolytes based on PVA/PVP blend with  $\text{MnCl}_2$  as the filler at different concentrations were prepared using a solvent casting technique.

XRD showed broad band which reveal the amorphous nature and that there are no new peaks appeared for  $\text{MnCl}_2$  indicating the complete dissolution of the filler in amorphous regions of polymer with decreasing in the crystallinity. FT-IR analysis manifested the conclusion about the specific interaction in polymer blend and hence the complexion and provides an insight into the possible interactions between  $\text{MnCl}_2$  and the polymers blend. The formation of intermolecular interactions and complexation between the PVA/PVP and the filler ( $\text{MnCl}_2$ ) was confirmed by XRD, FT-IR, UV-Vis. Optical absorption edge and optical band gaps (both direct and indirect) showed a decreasing trend with increased concentration of the  $\text{MnCl}_2$ . These data suggest that the present electrolyte system is a worthy candidate for electrochemical device applications. SEM shows a transparent, soft and a uniform pure PVA/PVP and it a smooth surface, while after adding the filler to the polymer by increasing the concentration a large granules and granule groups randomly distribution on the surface.

### REFERENCES

- [1] H.S.Lee, X.Q.Yang, J.McBreen, Z.S.Xu, T.A.Skotheim, Y.Okamoto; J.Electrochem.Soc., **141**, 886 (1994).
- [2] P.B.Bhargav, V.M.Mohan, A.K.Sharma, V.V.R.N.Rao; Curr.Appl.Phys., **9**, 165 (2009).
- [3] S.Zulfiqar, S.Ahmad; Polym.Degr.Stab., **65**, 24 (1999).
- [4] M.H.Abou Taleb; J.Appl.Polym.Sci., **114**, 1202 (2009).
- [5] S.H.Lim, S.M.Hudson; J.Macromol.Sci.Pol.R., **43**, 223 (2003).
- [6] V.Sedlarik, N.Saha, I.Kuritka, P.Saha; Polym.Compos., **27**, 147 (2006).
- [7] C.V.S.Reddy, X.Han, Q.Y.Zhu, L.Q.Mai, W. Chen; Microelectron.Eng., **83**, 281 (2006).

- [8] E.M.Abdelrazek, I.S.Elashmawi, S.Labeeb; *Physica B: Physics of Condensed Matter*, **405**, 2021 (2010).
- [9] E.M.Abdelrazek, I.S.Elashmawi, A.Yassin; *Current Appl.Phys.*, **10**, 607 (2010) .
- [10] F.Hassouna, S.Therias, G.Mailhot, J.Gardette; *Luc.Elsevier Ltd.*, **94**, 2257 (2008).
- [11] H.M.Ragab; *Physica B: Physics of Condensed Matter*, **406**, 3759 (2011).
- [12] J.L.Qiao, T.Hamaya, T.Okada; *Polymer*, **46**, 16 (2005).
- [13] S.Sethia, E.Squillante; *International Journal of Pharmaceutics*, **272**, 1 (2004).
- [14] I.S.Elashmawi, H.E.A.Baieth; *Current Applied Physics*, **12**, 141 (2012).
- [15] H.Wu, I.Wu, F.Chang; *Polym*, **42**, 555 (2001).
- [16] E.M.Abdelrazek, I.S.Elashmawi; *Polym.Compos.*, **29**, 1036 (2008).
- [17] W.H.Eisa, Y.K.Abdel-Moneam, A.A.Shabaka, A.E.M.Hosam; *Spectrochimic Acta Part (A) Mol and Biomol Spectroscopy*, **15**, 159 (2012).
- [18] M.M.El-Nahass, H.M.Zeyada, K.F.Abd-El-Rahman, A.A.M.Farag, A.A.A.Darwish; *Spectrochimica Acta Part A*, **69**, 205 (2008).
- [19] R.F.Bhajantri, V.Ravindrachary, B.Poojary, A.H.Ismayil, V.Crasta; *Polym.Eng.Sci.*, **574**,199 (2009).
- [20] E.M.Abdelrazek; *Physica B*, **403**, 2137 (2008).
- [21] G.Hirankumar, S.Selvasekarapandian, N.Kuwata, J.Kawamura, T.Hattori; *J.Power Sources*, **144**, 262 (2005).
- [22] G.M.Thutupalli, S.G.Tomlin; *J.Phys.D: Appl.Phys.*, **9**, 1639 (1976).
- [23] I.S.Elashmawi, N.A.Hakeem; *Polym.Eng.Sci.*, **895**, 48 (2008).
- [24] D.S.Davis, T.S.Shalliday; *Phys.Rev.*, **118**, 1020 (1960).
- [25] A.M.Abdelghany, H.A.ElBatal, L.Mari; *Radiation Effects and Defects in solids*, **167**, 49-58 (2012).